3Pb5-7

Significance of phase of transfer function in filter designed for high-resolution observation of muscle fiber

筋線維の高分解能観察のための filter 設計における伝達関数の位相特性の重要性

Kenta Kawamata[1‡], Shohei Mori[2], Mototaka Arakawa[1,2], and Hiroshi Kanai[2,1] ([1]Grad. School Biomed. Eng., Tohoku Univ.; [2]Grad. School Eng., Tohoku Univ.)

川又健太 [1‡], 森 翔平 [2], 荒川元孝 [1,2], 金井 浩 [2,1] ([1] 東北大院 医工, [2] 東北大院 工)

1. Introduction

For an accurate diagnosis of diseases with abnormal myocardial fibers such as ventricular noncompaction disease, real-time and non-invasive observation of myocardial fibers is essential and is also expected that new knowledge will be obtained in cardiac physiology. Since the spatial resolution of the conventional ultrasound diagnostic equipment is insufficient to observe the direction of myocardial fibers, it is necessary to broaden the bandwidth to improve the spatial resolution. In the present study, we examined the significance of the phase of the transfer function in the filter designed for broadening the frequency band.

2. Principles

Parametric Wiener filter (PWF)[1)]

Figure 1 shows a block diagram illustrating how to estimate the frequency spectrum $F_i(\omega)$ of the spatial distribution of the ultrasonic reflectivity of an object along i-th ultrasonic beam by Wiener filter $M(\omega)$. In Fig. 1, $G_i(\omega)$, $H(\omega)$, and $N(\omega)$ are the frequency spectra of the received echo from an object, the transfer function of the ultrasonic measurement system, and noise, respectively. We focus on the PWF given by

$$M(\omega) = \frac{1}{H(\omega)} \frac{|H(\omega)|^2}{|H(\omega)|^2 + \beta(\omega) \cdot \dfrac{P_\mathrm{N}(\omega)}{P_\mathrm{F}(\omega)}}, \quad (1)$$

where $P_\mathrm{N}(\omega)$ and $P_\mathrm{F}(\omega)$ are the averaged power spectra of noise component $N(\omega)$ and the true reflectivity $F_i(\omega)$. PWF can broaden only the frequency band with a high SN ratio, and the weight of SN ratio is controlled by the parameter $\beta(\omega)$. If $\beta(\omega) = 0$, PWF $M(\omega)$ behaves as an inverse filter $1/H(\omega)$.

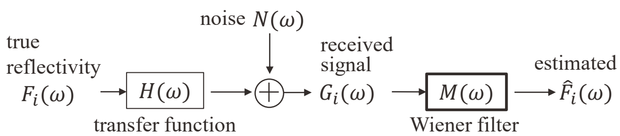

Fig. 1. Block diagram for estimating $\hat{F}_i(\omega)$ using Wiener filter $M(\omega)$.

k.kawamata@ecei.tohoku.ac.jp

3. Method

We previously designed the filters by focusing on the amplitude characteristics of the estimated signals[2)]. However, since the phase characteristics of the received RF signals also contain information of a measurement object, we designed the filters by focusing on the phase characteristics of the transfer function in the present paper.

We compared the results of applying the following two filters; (a) Wiener filter $M_\mathrm{h}(\omega)$ designed from the phase of the transfer function, $\angle H_\mathrm{h}(\omega)$, estimated using the hydrophone[2)], (b) Wiener filter $M_\mathrm{r}(\omega)$ designed by assuming uniform random phase as the phase of the transfer function, $\angle H_\mathrm{r}(\omega)$. Moreover, to focus only on the phase of the transfer function, we designed the filters so that $|\hat{F}_i(\omega)| = 1$: $\beta(\omega) = 0$ and $|H(\omega)| = |G(\omega)|$.

We measured the gastrocnemius muscle as a basic study since it is stationary for the measurement and is classified in striated muscle, which is the same as myocardium. We used the ultrasound diagnostic equipment (SSD-6500, Aloka) with a linear probe with a 7.5-MHz center frequency.

4. Results

Figure 2 shows the phases of the transfer function. Figure 2(a) is obtained by the hydrophone, and Fig. 2(b) shows the uniform random phase set in the experiment. **Figure 3** shows the B-mode images before and after applying each filter $M_\mathrm{h}(\omega)$ and $M_\mathrm{r}(\omega)$ to the received RF signals. **Figure 4** shows the amplitude and phase characteristics of the central beam (red line in Fig. 4) after applying each of the filters $M_\mathrm{h}(\omega)$ and $M_\mathrm{r}(\omega)$ to the received RF signals. As shown in Figs. 4(a)(i) and 4(b)(i), both amplitude characteristics $|\hat{F}_i(\omega)|$ were set to be 1 in the entire frequency range, so the difference between Figs. 3(b) and 3(c) was caused by only the difference of the phase characteristics $\angle\hat{F}_i(\omega)$.

In Fig. 3(c), which shows the result of applying the filter $M_\mathrm{r}(\omega)$ to the received RF signals, the B-mode image became a white-noise image. This is because the amplitude characteristics $|\hat{F}_i(\omega)|$ was equal to 1 in the entire frequency range and the phase characteristics $\angle H_\mathrm{r}(\omega)$ was a uniform random phase, therefore signal information of the object was lost in both of the amplitude characteristics $|\hat{F}_i(\omega)|$ and the phase characteristics $\angle\hat{F}_i(\omega)$.

On the other hand, in Fig. 3(b), which shows the result obtained by applying the filter $M_\mathrm{h}(\omega)$ to the received RF signals, some muscle fibers of the gastrocnemius can be observed with high brightness at a depth of about 3-12 mm. Although the amplitude characteristic is set to be 1 in the entire frequency range and the information on the amplitude characteristic of received signals was lost, we can observe the muscle fibers of the gastrocnemius using only the phase characteristics.

The reason that Fig. 3(b) was blurred compared to the original image in Fig. 3(a) is explained as follows: The amplitude characteristic $|\hat{F}_i(\omega)|$ was equal to 1 in the entire frequency range and therefore the high-frequency components were relatively amplified compared to before applying the filter $M_\mathrm{h}(\omega)$ to the received RF signals. This caused an increase in the noise level.

Also, in Fig. 3(b), the muscle fibers were not observed at a position deeper than the muscle boundary (deeper than about 12 mm). This is explained as follows: The reflection of ultrasonic waves was large at the muscle boundary and the power of ultrasonic waves became weak at points deeper than the muscle boundary, resulting in a lower SN ratio at a deeper position. Since the high-frequency components were amplified after applying the filter $M_\mathrm{h}(\omega)$, it is considered that the signals became lower than the noise level at positions deeper than the muscle boundary.

In the present study, to focus only on the phase characteristic, the amplitude characteristic $|\hat{F}_i(\omega)|$ was set to be 1 in the entire frequency range, however, it is expected that a better B-mode image can be obtained when the amplitude characteristic of the transfer function is accurately estimated.

5. Conclusion

In the present study, it was confirmed that even if the amplitude characteristics lost the signal information of the measurement target, the image information of the gastrocnemius muscle can be obtained using only the phase characteristics. Thus, the significance of the estimation of the phase $\angle H(\omega)$ of the transfer function was re-realized. In the future, we will study the phase $\angle H(\omega)$ of the transfer function and also use the amplitude characteristics of the received signal to design a filter more suitable for observing muscle fibers.

References

1. H. C. Andrews, and B. R. Hunt, Digital Image Resolution, Prentice-Hall, Inc, 1977.
2. S. Kageyama, H. Hasegawa, and H. Kanai, Jpn. J. Appl. Phys., **52**, 07HF04, 2013.

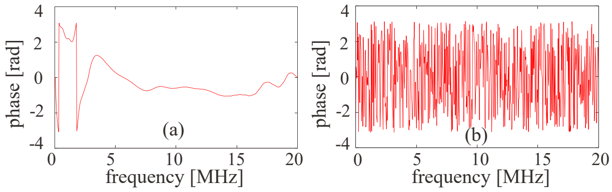

Fig. 2. The phases of transfer function, (a) $\angle H_\mathrm{h}(\omega)$ estimated using a hydrophone and (b) $\angle H_\mathrm{r}(\omega)$ assumed uniform random phase.

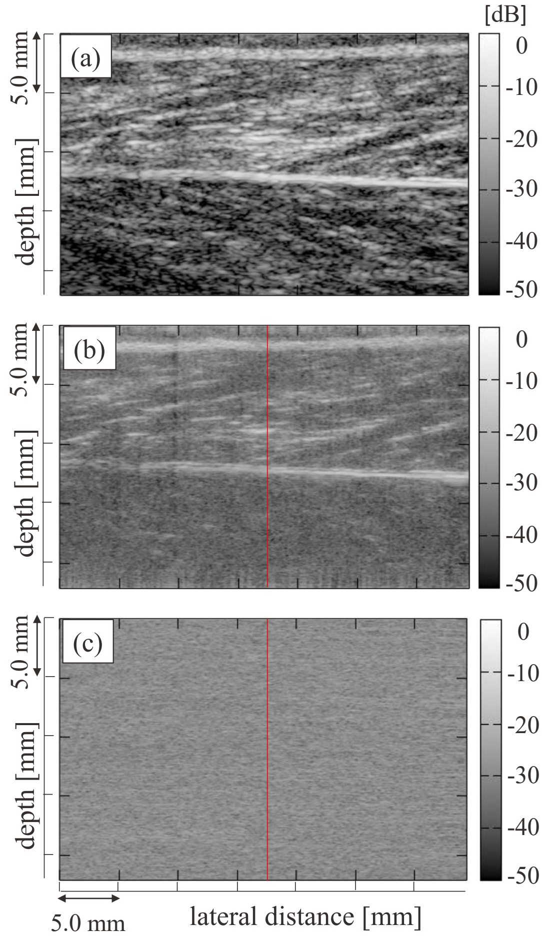

Fig. 3. B-mode images of gastrocnemius muscle, (a) before applying filter, (b) after applying filter $M_\mathrm{h}(\omega)$, and (c) after applying filter $M_\mathrm{r}(\omega)$.

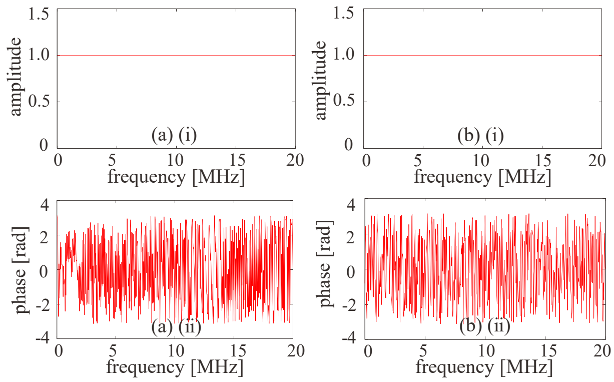

Fig. 4. (i) Amplitude $|\hat{F}_i(\omega)|$ and (ii) phase $\angle\hat{F}_i(\omega)$ after applying each filter (a) $M_\mathrm{h}(\omega)$ and (b) $M_\mathrm{r}(\omega)$.